Bioorganic & Medicinal Chemistry Letters 19 (2009) 3471–3475

Contents lists available at ScienceDirect

Bioorganic & Medicinal Chemistry Letters

journal homepage: www.elsevier.com/locate/bmcl

Hit-to-lead optimization of pyrrolo[1,2-*a*]quinoxalines as novel cannabinoid type 1 receptor antagonists

György Szabó [a,*], Róbert Kiss [a,b], Dóra Páyer-Lengyel [a], Krisztina Vukics [a], Judit Szikra [a], Andrea Baki [a], László Molnár [a], János Fischer [a], György M. Keserű [a]

[a] *Gedeon Richter Plc, Budapest 10, PO Box 27, H-1475, Hungary*
[b] *Department of Pharmaceutical Chemistry, Semmelweis University, Budapest, Högyes Endre u. 9., H-1092, Hungary*

ARTICLE INFO

Article history:
Received 10 April 2009
Revised 4 May 2009
Accepted 5 May 2009
Available online 7 May 2009

Keywords:
CB1 receptor
Rimonabant
Hit-to-lead
SAR
Pyrrolo[1,2-*a*]quinoxaline

ABSTRACT

Hit-to-lead optimization of a novel series of *N*-alkyl-*N*-[2-oxo-2-(4-aryl-4*H*-pyrrolo[1,2-*a*]quinoxaline-5-yl)-ethyl]-carboxylic acid amides, derived from a high throughput screening (HTS) hit, are described. Subsequent optimization led to identification of in vitro potent cannabinoid 1 receptor (CB1R) antagonists representing a new class of compounds in this area.

According to the WHO Global InfoBase, 78% of the population of United States and 73% of the United Kingdom is classified as obese or overweight. Moreover, it is not only western society that is affected as the prevalence of obesity has increased worldwide by 75% since 1980 and the WHO have consequently defined it as a global epidemic.[1] The discovery of the endocannabinoid system, in the 90s, has provided a novel opportunity to develop and introduce efficient pharmaceuticals for the treatment of obesity.[2] The endocannabinoid system, and the CB1 receptor (cloned in 1990)[3] in particular, plays a special role in energy homeostasis. Blockade of CB1 receptors decreases food intake leading to a reduction in body weight. Therefore, it was hoped that CB1 receptor antagonists/inverse agonists could provide effective therapies for the treatment of obesity.[4,5] Unfortunately, rimonabant[6] (SR141716A), the first potent and selective CB1 receptor inverse agonist (Fig. 1) was recently reported to cause serious psychiatric side-effects.[7] Consequently, several CB1 antagonists (including taranabant[8] (MK-0364) and otenabant[9] (CP-945,598)) were withdrawn from the market and/or clinical development. Whether these side effects arise from the mechanism of action itself or they are compound specific remains uncertain. It is therefore important to identify and develop novel structures that may provide a distinct therapeutic profile.

Herein, the discovery and hit-to-lead optimization of a novel series of CB1 receptor antagonists, *N*-alkyl-*N*-[2-oxo-2-(4-aryl-4*H*-pyrrolo[1,2-*a*]quinoxaline-5-yl)-ethyl]-carboxylic acid amides, are described.

An in-house high throughput screening (HTS) campaign using a functional Ca^{2+} assay[10] yielded several hits featuring a pyrrolo[1,2-*a*]quinoxaline core, as represented by compound **11** (Fig. 2).

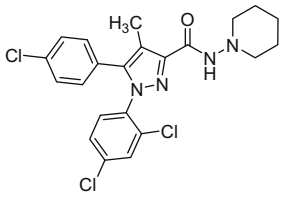

Figure 1. Structure of rimonabant **1**.

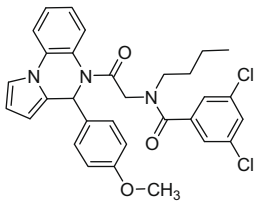

Figure 2. The original HTS hit, compound **11**.

* Corresponding author. Tel.: +36 1 481 5180; fax: +36 1 432 6979.
E-mail address: gy.szabo@richter.hu (G. Szabó).

0960-894X/$ - see front matter © 2009 Elsevier Ltd. All rights reserved.
doi:10.1016/j.bmcl.2009.05.010

Compound **11** displayed submicromolar affinity for the CB1 receptor (K_i = 831 nM), our efforts were therefore focused on the hit-to-lead optimization and structure–activity relationship (SAR) development of the pyrrolo[1,2-*a*]quinoxaline template to identify compounds with improved in vitro affinity.

In order to improve the potency of compound **11**, three areas were addressed: (R) the effect of the alkyl side chain, (R^1) the effect of acyl groups, and (R^2) the effect of groups of the pyrrolo-quinoxaline ring.

A general synthetic strategy of *N*-alkyl-*N*-{2-oxo-2-[4-(4-methoxy-phenyl)-4*H*-pyrrolo[1,2-*a*]quinoxaline-5-yl]-ethyl}-carboxylic acid amide analogues is illustrated in Scheme 1. Starting from commercially available 1-(2-aminophenyl)-pyrrole **2**, cyclization with *p*-methoxy-benzaldehyde in the presence of a catalytic amount of acetic acid in ethanol gave dihydro-pyrrolo[1,2-*a*]quinoxaline **3**, which could be easily converted to the acetylated product **4** using triethylamine (TEA) and dichloromethane (DCM) as solvent. A facile two-step protocol involving an alkylation followed by an acetylating step (using the appropriate carboxylic acid chloride in the presence of TEA or using the carboxylic acid in the presence of dicyclohexylcarbodiimide (DCC)) provided rapid access to the desired products **11–27** bearing structural variations in the R and R^1 positions.

The synthesis of compounds **39–45** containing different R^2 substituents were accomplished according to the procedures depicted in Scheme 2. The key intermediate **31** required for the synthesis was obtained in three steps. Ethyl-bromoacetate **28** was treated with *n*-butylamine in toluene at room temperature to afford amine **29** in a yield of 90%. Compound **30** was synthesized via acetylating of **29** using 2-chloro-acetyl chloride in the presence of TEA. Alkaline hydrolysis of ester **30** readily produced the expected intermediate **31**. Compounds **32–38** were obtained in a similar method as described for compound **3** in Scheme 1. Target compounds **39–45** were obtained by parallel synthesis via amidations of **32–38** with intermediate **31** using polymer-supported DCC in dry DCM. The IR, ^{1}H NMR, ^{13}C NMR and MS spectra for all the synthesized intermediates and final compounds were consistent with the assigned structures. Moreover, the purity of compounds was checked by HPLC and LCMS.

We began with modification of R^1 to reduce the molecular weight (MW), therefore, initial efforts focused on replacing the halogen substituents and/or removing the phenyl ring. As shown in Table 1 replacing the halogen substituents increased the potency as the substituents of the phenyl ring were in the *ortho*-position (compounds **16**, **17**, **18**). In order to further reduce the MW we prepared a series of cycloalkyl and alkyl derivatives. As shown, lower cycloalkyl ring size afforded better potency, while replacing the phenyl ring by a methyl group led to a total loss of potency (**24**). Interestingly, introducing a chloroethyl substituent led to an 18-fold increase in efficacy (compound **27**, K_i = 46 nM).

With the result of compound **27** in hand, we next focused on the R substituent. Removal of the butyl group in **27**, potency is lost. The same results were obtained when smaller alkyl, *i*-alkyl or cycloalkyl groups were used, the potency lost (**13**, **15**) or resulted in a drastic drop in efficacy (**14**). To further optimize the potency of **27**, we investigated the role of R_1 substituents. Simple methyl (**41**) or ethyl (**42**) derivative of **27** led to a complete loss of activity, indicating the importance of bulky substituents at this position that can be accommodated at the binding site. The *para*-position of the phenyl ring is preferred, as the *ortho*- (**39**) and disubstituted

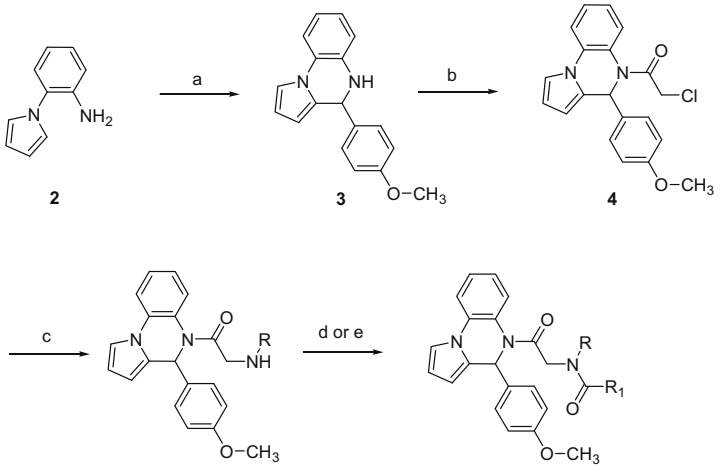

Scheme 1. Reagents and conditions: (a) *p*-methoxy-benzaldehyde, CH_3COOH, EtOH, 50 °C; (b) $ClCH_2COCl$, Et_3N, CH_2Cl_2, 0–5 °C; (c) R^1NH_2, CH_3CN, K_2CO_3, 60 °C; (d) RCOCl, Et_3N, CH_2Cl_2, 0–5 °C; (e) RCOOH, DCC, CH_2Cl_2.

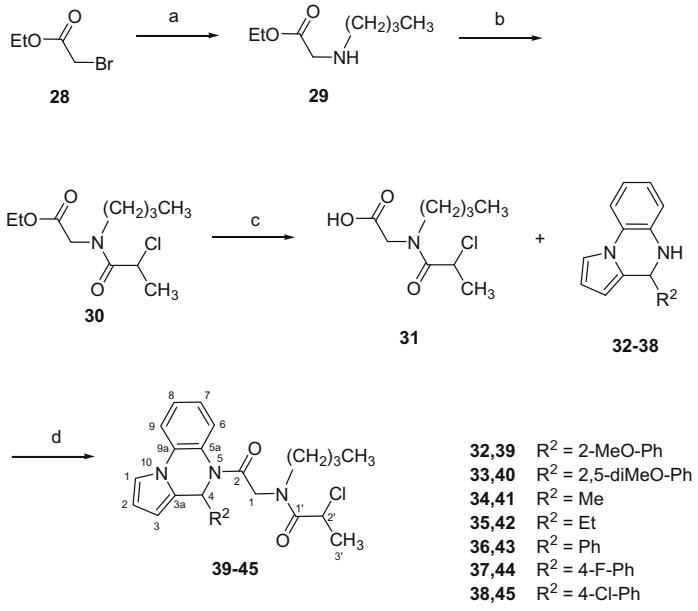

Scheme 2. Reagents and conditions: (a) *n*-butylamine, toluene, rt; (b) $CH_3CH(Cl)COCl$, Et_3N, CH_2Cl_2, 0–5 °C; (c) KOH, MeOH, rt; (d) PS-DCC, CH_2Cl_2, rt.

Table 1
Biological assay results for compounds **11**–**27** and **39**–**45**

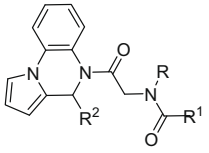

Cmpds	R	R^1	R^2	*n*	CB1 assay[a] Inh (%)[b], K_i (nM)
11	Butyl	3,5-DiCl-phenyl	4-MeO-Ph	1	831
12	H	$CH(CH_3)Cl$	4-MeO-Ph	1	25%
13	CH_3	$CH(CH_3)Cl$	4-MeO-Ph	1	46%
14	*i*-Propyl	$CH(CH_3)Cl$	4-MeO-Ph	3	220 ± 32
15	Cyclo-propyl	$CH(CH_3)Cl$	4-MeO-Ph	1	40%
16	Butyl	2-Cl-phenyl	4-MeO-Ph	1	137
17	Butyl	2-Me-Ph	4-MeO-Ph	1	503
18	Butyl	2-F-Ph	4-MeO-Ph	3	349 ± 94
19	Butyl	*i*-Butyl	4-MeO-Ph	3	236 ± 0.9
20	Butyl	Cyclopentyl	4-MeO-Ph	3	602 ± 4.7
21	Butyl	Cyclobutyl	4-MeO-Ph	3	214 ± 8.0
22	Butyl	Cyclopropyl	4-MeO-Ph	3	78 ± 10
23	Butyl	$CH(CH_3)_2$	4-MeO-Ph	3	124 ± 24
24	Butyl	CH_3	4-MeO-Ph	1	31%
25	Butyl	CH_2CH_3	4-MeO-Ph	3	539 ± 118
26	Butyl	CH_2OMe	4-MeO-Ph	3	461 ± 83
27	Butyl	$CH(CH_3)Cl$	4-MeO-Ph	3	46 ± 1.0
39	Butyl	$CH(CH_3)Cl$	2-MeO-Ph	1	36%
40	Butyl	$CH(CH_3)Cl$	2,5-DiMeO-Ph	1	45%
41	Butyl	$CH(CH_3)Cl$	CH_3	1	15%
42	Butyl	$CH(CH_3)Cl$	CH_2CH_3	1	14%
43	Butyl	$CH(CH_3)Cl$	Ph	3	260 ± 9.4
44	Butyl	$CH(CH_3)Cl$	4-F-Ph	3	162 ± 13
45	Butyl	$CH(CH_3)Cl$	4-Cl-Ph	3	45 ± 7.1
1				5	6.5 ± 0.8

[a] CB1 receptor affinity of the compounds was determined using rat cerebellum membrane preparation and [^{3}H]SR141716A.[11] Values represent means ± S.E.M. The number of experiments (*n*) is indicated.
[b] Inh % was obtained using 1 μM concentration of compounds.

analogues (**40**) were inactive. Simple substituents such as halogens were well tolerated at this position, yielding compound **45** with comparable in vitro potency to that of compound **27**.

The binding mode of one of the most potent compound of the pyrrolo-quinoxaline series (compound **45** in Table 1) was analyzed by docking calculations. A novel human CB1 receptor (hCB1R) homology model was developed by using the recently solved crystal structure of the human β2 adrenergic receptor (hβ2AR) (PDB ID: 2RH1).[12] Automated sequence alignment was carried out by ClustalW 2.0.10.[13] with the amino acid sequences of hCB1R and hβ2AR. Manual adjustments were applied by using the information available on conserved GPCR residues. 100 preliminary homology

models were generated by Modeller 9v6.[14] The best model indicated by the Modeller Objective Function was selected for further studies. Next, validation tests were carried out to verify the quality of this model. Procheck[15] and Whatif[16] tests indicated that the model is of acceptable quality, no problematic residues were observed at the binding site. Moreover, all residues reported to be important for ligand binding faced to the interior of the binding site.

The best preliminary model was prepared for docking using the Protein Preparation Wizard available in MAESTRO.[17] Rimonabant was prepared for docking by LIGPREP,[18] and it was subsequently docked to the binding site of our hCB1R homology model by GLIDE[19] in standard precision (SP) mode. The best docking pose represented a conformation where rimonabant formed strong lipophilic interactions with aromatic residues at the binding site.

Furthermore, rimonabant was in a favorable orientation to form an H-bond with Lys192 (3.28). On the other hand, the conformation of the side chain of Lys192 (3.28) was suboptimal for a strong interaction.

Therefore, 5000 steps Polak-Ribiere-type conjugate gradient energy optimization was carried out with the OPLS_2005 force field[20] by MacroModel available in MAESTRO.[17] Since the role of Lys192 (3.28) in rimonabant binding was already proved by site-directed mutagenesis,[21] a distance constraint between the side chain N atom of Lys192 (3.28) and the carbonyl O atom was applied with a harmonic potential (force constant = 100 kJ/mol Å^2). As a result, an optimized hCB1R-rimonabant complex was obtained including a strong H-bond between the carbonyl oxygen atom of rimonabant and Lys192 (3.28) (Fig. 3A).

In addition, rimonabant formed several lipophilic interactions with the binding site. The two phenol rings and the pyrazole ring of rimonabant accommodated favorably in a lipophil pocket composed by Phe170 (2.57), Leu193 (3.29), Val196 (3.32), Phe200 (3.36), Pro269 (5.33), Ile271 (5.35), Tyr275 (5.39), Trp279 (5.43), Trp356 (6.48), Leu359 (6.51) and Phe379 (7.35). The piperidine ring was surrounded by Ile175 (2.62), His178 (2.65), Val179 (2.66), Pro269 (5.33) and Phe379 (7.35). These results are in line with the mutagenesis data reported by McAllister et al.[22] These authors found that mouse CB1 binding affinity of rimonabant was significantly reduced by Phe201(3.36)Ala, Trp280(5.43)Ala and Trp357(6.48)Ala mutations. On the other hand, no significant affinity drop was observed in the case of Phe190(3.25)Ala mutation. The optimized complex is also in agreement with the mutagenesis data published by Kapur et al.,[23] that is, rimonabant did not form interaction with either Ser383 (7.39) or Ser173 (2.60).

Next, we docked the most potent compound of the newly discovered pyrrolo-quinoxaline series (compound **45**) to the hCB1R binding site. Since compound **45** contains two chiral centers, and CB1 binding affinity data were obtained only for the racemic form, all four possible stereoisomers were prepared for docking by LIGPREP.[18] All stereoisomers were docked to the binding site, but GLIDE has found potential docking conformation for one stereoisomer only (2′*S*,4*R*). Consequently, we suggest that this stereoisomer is responsible for the high CB1 affinity. GLIDE yielded a reasonable binding conformation for compound **45**, where the ring system occupied a similar position as rimonabant. Energy optimization of the complex was carried out as described above without any constraints. In the resulting optimized structure, one of the carbonyl oxo groups formed an H-bond with Ser383 (7.39). This residue was previously reported to be crucial for taranabant binding.[24] Moreover, the other carbonyl oxygen got into a favorable orientation to form an H-bond with Lys192 (3.28), but similarly to the case of rimonabant, the conformation of Lys192 (3.28) was suboptimal for a strong interaction. Therefore a second energy optimization was carried using a distance constraint between the appropriate oxygen of compound **45** and the side chain nitrogen of Lys192 (3.28). This resulted in a complex with two strong H-bonds with Ser383 (7.39) and Lys192 (3.28) (Fig. 3B). The 4-chlorophenyl group of compound **45** formed lipophil interactions with Ile271 (5.35), Phe268 (5.32), Pro269 (5.33) and Phe379 (7.35). The pyrrolo-quinoxaline ring system fitted favorably to the lipophil pocket comprised by Ile271 (5.35), Leu193 (3.29), Phe170 (2.57), Val196 (3.32), Tyr275 (5.39), Trp279 (5.43), Phe200 (3.36), Trp356 (6.48) and Leu359 (6.51). The butyl side chain was surrounded by Phe268 (5.32), Phe379 (7.35) and Ala380 (7.36), while the 1-chloroethyl group formed lipophil interactions with Ile175 (2.62), His178 (2.65), Val179 (2.66). In summary, compound **45** was found to possess a similar binding conformation to that of rimonabant, but an additional H-bond with Ser383 (7.39) was also observed.

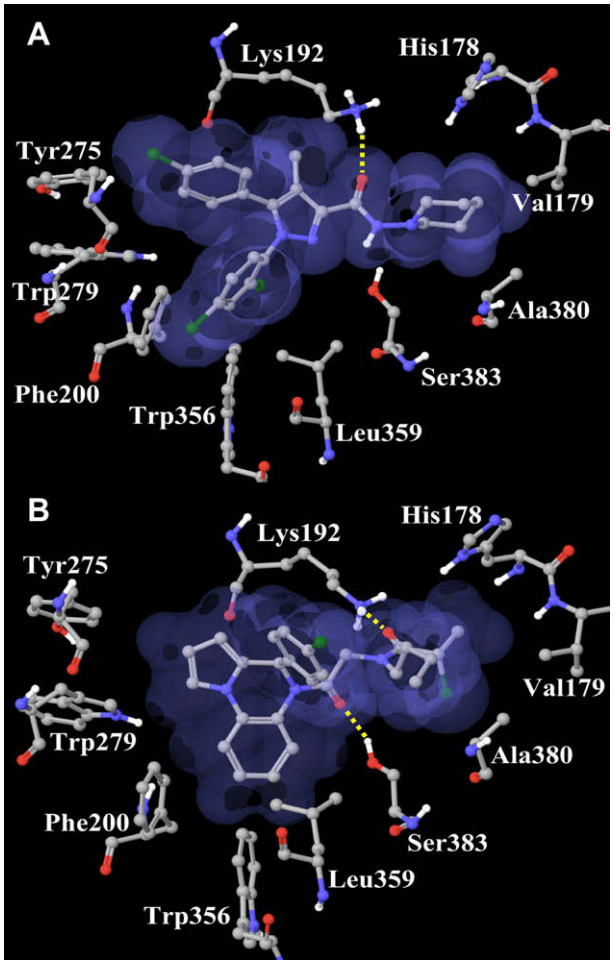

Figure 3. Binding mode of rimonabant (A) and compound **45** (B). Important residues and the ligands are represented as 'ball and sticks'. Van der Waals surfaces of the ligands are shown in light blue. H-bonds are shown as yellow dotted lines. Some residues are omitted for clarity.

In conclusion, a new class of CB1 antagonist compounds has been described and tested for CB1 receptor binding affinities. Preliminary hit-to-lead optimization of the series has led to compounds such as **45**, which shows significant in vitro activity. The investigation of the binding mode of **45** revealed similar binding mode to that of rimonabant. Further optimization and application of this series of compounds will be reported in due course.

References and notes

1. Bray, G. A. *J. Med. Chem.* **2006**, *49*, 4001.
2. Di Marzo, V.; Bifulco, M.; De Petrocellis, L. *Nat. Rev. Drug Disc.* **2004**, *3*, 771.

3. Matsuda, L. A.; Lolait, S. J.; Brownstein, M. J.; Young, A. C.; Bonner, I. *Nature* **1990**, *346*, 561.
4. Pagotto, U.; Vicennati, V.; Pasquali, R. *Ann. Med.* **2005**, *37*, 270.
5. Pertwee, R. G. *Int. J. Obesity* **2006**, *30*, 513.
6. Rinaldi-Carmona, M.; Barth, F.; Héaulme, M.; Shire, D.; Calandra, B.; Congy, C.; Martinez, S.; Maruani, J.; Néliat, G.; Caput, D. *FEBS Lett.* **1994**, *350*, 240.
7. Bellocchio, L.; Mancini, G.; Vicennati, V.; Pasquali, R.; Pagotto, U. *Curr. Opin. Pharmacol.* **2006**, *6*, 586.
8. Lin, L. S.; Lanza, T. J., Jr.; Jewell, J. P.; Liu, P.; Shah, S. K.; Qi, H.; Tong, X.; Wang, J.; Xu, S. S.; Fong, T. M.; Shen, C. P.; Lao, J.; Xiao, J. C.; Shearman, L. P.; Stribling, D. S.; Rosko, K.; Strack, A.; Marsh, D. J.; Feng, Y.; Kumar, S.; Samuel, K.; Yin, W.; Van der Ploeg, L. H.; Goulet, M. T.; Hagmann, W. K. *J. Med. Chem.* **2006**, *49*, 7584.
9. Griffith, D. A.; Hadcock, J. R.; Black, S. C.; Iredale, P. A.; Carpino, P. A.; DaSilva-Jardine, P.; Day, R.; DiBrino, J.; Dow, R. L.; Landis, M. S.; O'Connor, R. E.; Scott, D. O. *J. Med. Chem.* **2009**, *52*, 234.
10. The CB1 HTS intracellular fluorometric Ca^{2+} assay was performed on the CHO-K1 cell line stably expressing the cloned human CB1 receptor and Gα16 protein (Euroscreen s.a., Belgium, Cat. No: ES-110-F). Cells grown in ultraCHO medium without antibiotics were loaded with equal volume of loading buffer (20 μl) and were incubated for 1 h at 37 °C. 10 μl of test compounds were added and the plates were incubated for 10 min at room temperature. The intracellular Ca^{2+} measurement was performed in the FLIPR Tetra and it was initiated by adding 10 μl of agonist (CP 55,940). The concentration–effect relationship for CP 55,940 was determined every day, prior to the test. For HTS purpose we used the $2 \times EC_{80}$ agonist concentration. The final reaction volume was 60 μl and the final DMSO concentration was set to be 0.9%.
11. In vitro [^{3}H]SR141716A ligand binding at CB1 receptors. Rat cerebellum was removed and homogenized and a membrane preparation was stored at −80 °C until use. A solution of 0.4 nM [^{3}H]SR-141716A in 50 mM Tris–HCl buffer complemented with 5 mM $MgCl_2$, 1 mM EDTA and containing 20% ethanol was prepared freshly each day from a stock solution (0.002 mCi/ml, in ethanol). Incubation was performed in the above-mentioned buffer complemented with 1 mg/ml bovine serum albumin (BSA) and 1 mM dithiothreitol (DTT) for 60 min at 30 °C in a thermostated shaker. Incubation mixture (total volume of 1 ml) contained 200 μg rat cerebellar membrane (thoroughly homogenized and kept vortexed under the whole preincubation procedure) while the final radioligand concentration was 0.04 nM. Assay mixture was then filtered through Whatman GF/C glass fiber filters (Brandel M48 harvester) and washed with 5 × 5-ml incubation buffer (without DTT). Filters were dried and placed in scintillation vials and 3.5 ml HiSafe scintillation cocktail was added. Samples were left to stand for overnight and radioactivity was determined in a Wallac 1409 scintillation spectrometer. Non-specific binding was determined in the presence of 1 μM unlabeled SR141716A. IC_{50} values were determined from displacement curves using sigmoid fitting by Origin 6.0 software. K_i values were calculated by the Cheng–Prusoff equation.
12. Cherezov, V.; Rosenbaum, D. M.; Hanson, M. A.; Rasmussen, S. G.; Thian, F. S.; Kobilka, T. S.; Choi, H. J.; Kuhn, P.; Weis, W. I.; Kobilka, B. K.; Stevens, R. C. *Science* **2007**, *318*, 1258.
13. Thompson, J. D.; Higgins, D. G.; Gibson, T. J. *Nucleic Acids Res.* **1994**, *22*, 4673.
14. Sali, A.; Blundell, T. L. *J. Mol. Biol.* **1993**, *234*, 779.
15. Laskowski, R. A.; MacArthur, M. W.; Moss, D. S.; Thorton, J. M. *J. Appl. Crystallogr.* **1993**, *26*, 283.
16. Vriend, G.; Sander, C. *J. Appl. Crystallogr.* **1993**, *26*, 47.
17. MAESTRO, *Version 8.5*; Schrodinger: New York, NY, 2008.
18. LIGPREP, *Version 2.2*; Schrodinger: New York, NY, 2008.
19. GLIDE, *Version 5.0*; Schrodinger: New York, NY, 2008.
20. Jorgensen, W. L.; Maxwell, D. S.; Tirado-Rives, J. *J. Am. Chem. Soc.* **1996**, *118*, 11225.
21. Hurst, D. P.; Lynch, D. L.; Barnett-Norris, J.; Hyatt, S. M.; Seltzman, H. H.; Zhong, M.; Song, Z. H.; Nie, J.; Lewis, D.; Reggio, P. H. *Mol. Pharmacol.* **2002**, *62*, 1274.
22. McAllister, S. D.; Rizvi, G.; Anavi-Goffer, S.; Hurst, D. P.; Barnett-Norris, J.; Lynch, D. L.; Reggio, P. H.; Abood, M. E. *J. Med. Chem.* **2003**, *46*, 5139.
23. Kapur, A.; Hurst, D. P.; Fleischer, D.; Whitnell, R.; Thakur, G. A.; Makriyannis, A.; Reggio, P. H.; Abood, M. E. *Mol. Pharmacol.* **2007**, *71*, 1512.
24. Lin, L. S.; Ha, S.; Ball, R. G.; Tsou, N. N.; Castonguay, L. A.; Doss, G. A.; Fong, T. M.; Shen, C. P.; Xiao, J. C.; Goulet, M. T.; Hagmann, W. K. *J. Med. Chem.* **2008**, *51*, 2108.